Journal of Sound and Vibration 329 (2010) 2547–2564

Contents lists available at ScienceDirect

Journal of Sound and Vibration

journal homepage: www.elsevier.com/locate/jsvi

Nonlinear vibration of micromachined asymmetric resonators

Pezhman A. Hassanpour [a,*], Ebrahim Esmailzadeh [b], William L. Cleghorn [c], James K. Mills [c]

[a] Department of Mechanical and Mechatronics Engineering, University of Waterloo, Waterloo, Ontario, Canada N2L 3G1
[b] Faculty of Engineering and Applied Science, University of Ontario Institute of Technology, Oshawa, Ontario, Canada L1H 7K4
[c] Department of Mechanical and Industrial Engineering, University of Toronto, Toronto, Ontario, Canada M5S 3G8

ARTICLE INFO

Article history:
Received 7 April 2009
Received in revised form
25 September 2009
Accepted 26 October 2009
Handling Editor: M.P. Cartmell
Available online 10 February 2010

ABSTRACT

In this paper, the nonlinear dynamics of a beam-type resonant structure due to stretching of the beam is addressed. The resonant beam is excited by attached electrostatic comb-drive actuators. This structure is modeled as a thin beam-lumped mass system, in which an initial axial force is exerted to the beam. This axial force may have different origins, e.g., residual stress due to micro-machining. The governing equations of motion are derived using the mode summation method, generalized orthogonality condition, and multiple scales method for both free and forced vibrations. The effects of the initial axial force, modal damping of the beam, the location, mass, and rotary inertia of the lumped mass on the free and forced vibration of the resonator are investigated. For the case of the forced vibration, the primary resonance of the first mode is investigated. It has been shown that there are certain combinations of the model parameters depicting a remarkable dynamic behavior, in which the second to first resonance frequencies ratio is close to three. These particular cases result in the internal resonance between the first and second modes. This phenomenon is investigated in detail.

1. Introduction

Micro-resonators are the building blocks of many micro-electromechanical systems (MEMS), e.g., micro-gyroscopes and resonant sensors. Due to the oscillatory nature of these devices, dynamics of micro-resonators has been an interesting field for researchers. Among many different resonators, micro-bridges are one of the most frequently used structures. A micro-bridge is essentially a beam clamped at both ends.

Fig. 1 shows a resonant micro-bridge with two attached comb-drives for the excitation and detection of vibration of the resonant beam. This structure can be used for resonant sensing, because the natural frequencies of the beam are functions of its axial load. One of the attached comb-drives is used to oscillate the resonator, while the other is for sensing the vibration.

Fig. 2 shows the schematic of an electrostatic comb-drive actuator. The force applied to the beam laterally can be expressed as [1]

$$F = \frac{\varepsilon_0 N h}{2g} V^2, \tag{1}$$

* Corresponding author.
E-mail addresses: hassanpr@mme.uwaterloo.ca, pezhman.hassanpour@gmail.com (P.A. Hassanpour).

0022-460X/$ - see front matter Crown Copyright © 2010 Published by Elsevier Ltd. All rights reserved.
doi:10.1016/j.jsv.2009.10.033

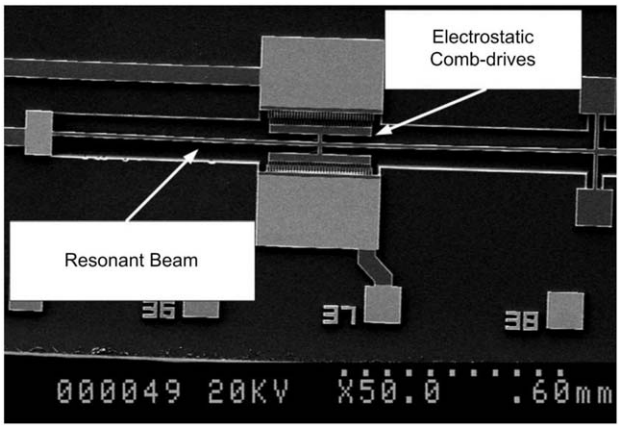

Fig. 1. SEM of a resonant beam with attached comb-drives.

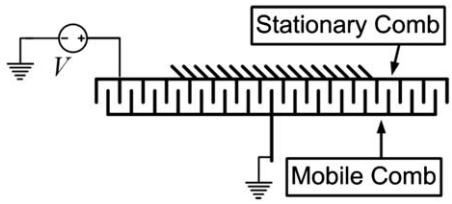

Fig. 2. Schematic of an electrostatic comb-drive actuator.

where ε_0 is the permittivity of free space; N is the number of fingers; h is the MEMS structural layer thickness; g is the gap between two consecutive stationary and mobile fingers; and V is the applied voltage. The electrostatic force usually ranges from a few nano-Newtons to a few hundreds of micro-Newtons, depending on the dimensions of the structure.

In the device shown in Fig. 1, the comb-drives are located at the mid-point of the beam; therefore, the motion of the system is symmetric with the main contribution from the fundamental mode of vibration. Hence, a single degree-of-freedom model (SDOF), i.e., mass-spring-damper, can be used to model this system. The stiffness of the spring will be the stiffness of the beam at the mid-point, i.e., $k = 192EI/L^3$ [1], while the mass will be the mass of the comb-drive. In those cases where the mass of the beam is comparable to the mass of the combs, the beam's effective mass can be taken into account as well.

When the mass of the beam is large compared to the mass of the combs, or the natural frequencies and responses of the system at higher modes of vibration is desired, SDOF models are no longer adequate. In these cases, a continuous model should be used. Hassanpour et al. [2] assumed that the dimensions of the combs were small compared to those of the beam; therefore, the combs could be modeled as a point mass, i.e., a mass with no rotary inertia. They also assumed that the position of the point mass was arbitrary on the beam. Using the thin beam theory and considering the effect of the axial force, they investigated the effect of axial force, mass ratio, and location on the natural frequencies and mode shapes of the beam. These results showed that the rotation of the point mass was not negligible; hence, the effect of rotary inertia of the combs must be taken into account, in general.

As an extension to their previous model, Hassanpour et al. [3] took into account the rotary inertia of the combs. They showed that although the inertia of the resonator was increased by the mass of the comb-drives, its natural frequencies could be higher than those of the original beam by properly positioning the combs on the resonant beam. This new structure is called an *asymmetric resonator* [4]. It has been shown that the electrostatic comb-drives in an asymmetric resonator are stable and robust to rocking motions, thanks to the resistance to rotation imposed to the beam by their rotary inertia [3,4].

As mentioned earlier, many MEMS devices are based on dynamic effects. In some cases, these devices are controlled to remain in the linear regime. In other cases, the nonlinearity is either desirable, or inevitable. Various forms of nonlinear dynamic behavior have been already observed experimentally [5–12]. Bahreyni and Shafai [13] used a symmetric beam with two attached comb-drives to measure the intensity of the magnetic field. They have observed that by increasing the amplitude of vibration, the response of the system depicts nonlinear behavior [14]. This phenomenon can be explained by noting that a large deflection causes the axial stretching of the beam, which in turn produces a tensile axial force. Therefore, the magnitude of this axial force is a function of the amplitude of deflection. It must be noted that a micro-bridge might be under an initial constant axial force, which can be either tensile or compressive.

Ozkaya et al. [16,17] and Low [18] have investigated the nonlinear vibration of a thin beam carrying a point mass for the boundary conditions of pinned–pinned, pinned–guided, guided–guided, pinned–clamped, and guided–clamped ends. These studies include the application of the method of multiple scales for solving the nonlinear equations, while excluding the effect of rotary inertia of the point mass as well as the effect of the initial axial force in the beam. Moreover, the first five modes of linear vibration for different cases are calculated, however, only the fundamental mode has been used to derive the nonlinear frequency versus amplitude of vibration. It has been shown that using exact higher modes requires the application of the generalized orthogonality condition [19]. Ozkaya and Pakdemirli [21] have used the exact fundamental mode shape of a beam-point mass system clamped at both ends. This study does not include the effect of the rotary inertia of the mass and the initial axial force in the beam. Ozkaya [22] has modeled the nonlinear vibration of a simply supported beam carrying several point masses at its interval, neglecting the initial axial force in the beam, rotary inertia of the point masses, as well as the effect of second and higher modes in the nonlinear vibration. The nonlinear vibrations of beams with non-ideal supports have been studied in Ref. [23]. The nonlinear dynamics of a stepped beam has been studied in Ref. [24]. Ramezani et al. [25] have modeled the effects of rotary inertia and shear deformation of the beam, itself, on nonlinear free vibration of micro-beams. Vyas et al. [26] have modeled the internal resonance between an out-of-plane torsional mode and a flexural in-plane vibrating mode.

As mentioned earlier, the beam-lumped mass systems can be used as the building blocks of resonant sensors. In these systems, the initial axial force in the beam is the key quantity to be measured, and cannot be neglected at all. Moreover, it has been shown that this axial force along with the lumped mass ratio, radius of gyration, and location change the exact mode shapes of vibration. These exact mode shapes are no longer orthogonal to each other under the conventional definition of orthogonality, but a generalized form of orthogonality condition that takes into account the effects of the lumped mass must be used. Due to the modification of the mode shapes of the beam-lumped mass system, the stretching of the beam must be revisited as it is a function of the mode shapes. In addition, asymmetric beam-lumped mass systems have a remarkable feature: frequency ratio tunability. The ratios between the natural frequencies of a beam are fixed, and determined as soon as the boundary conditions of that beam are set. For example, the second to first natural frequency ratio of a micro-bridge, i.e., a clamped–clamped beam, is approximately equal to 2.7565 regardless of its dimensions [27]. This ratio for a cantilever beam is roughly 6.2669 [27]. For a beam-lumped mass resonator, this ratio can be easily changed by adjusting the properties of the lumped mass as well as the beam initial axial force. This feature brings a vast opportunity to designers to exploit nonlinear dynamics in realizing innovative devices.

In this paper, the model of a beam-lumped mass system is adopted for studying the system of a micro-bridge with attached electrostatic comb-drives. This model includes the effect of the initial axial force in the beam and stretching due to large deflections. The nonlinear problem is formulated using the method of multiple scales. In contrast to previous studies, first and higher modes of vibration are used by the application of the generalized orthogonality condition. The free nonlinear vibration equation is solved to determine the shift of the natural frequencies in terms of the amplitude of vibration. The primary resonance of the system is investigated, once for the general case, and once for those particular cases in which the second natural frequency is tuned to be approximately three times of the fundamental natural frequency. It has been shown that this particular situation triggers an internal resonance. For each section of the modeling, the effects of contributing parameters are discussed in detail.

2. Analytical model

Fig. 3 shows the model of the resonant beam with electrostatic comb-drives for vibration excitation and detection. Assuming that the beam carrying the axial force is straight initially, and neglecting its shear deformation and rotary inertia, the governing equation of motion can be derived as [15,28]

$$\rho A\hat{W}_{\hat{t}\hat{t}} + M\hat{W}_{\hat{t}\hat{t}}(L_L,\hat{t})\hat{\delta}(\hat{x}-L_L) - J\hat{W}_{\hat{x}\hat{t}\hat{t}}(L_L,\hat{t})\hat{\delta}'(\hat{x}-L_L) - \hat{P}\hat{W}_{\hat{x}\hat{x}} + EI\hat{W}_{\hat{x}\hat{x}\hat{x}\hat{x}}$$
$$= (EA-\hat{P})\frac{\partial}{\partial\hat{x}}\left[\left(\frac{1}{2L}\int_0^L \hat{W}_{\hat{x}}^2\,\mathrm{d}\hat{x}\right)\hat{W}_{\hat{x}}\right] + F(\hat{t})\hat{\delta}(\hat{x}-L_L), \tag{2}$$

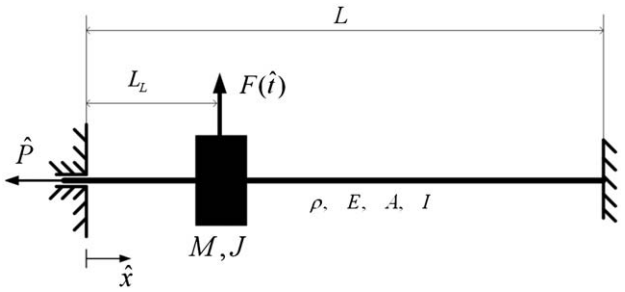

Fig. 3. Model of a clamped–clamped beam with attached lumped mass.

where ρ is the density, E is the modulus of elasticity, A is the cross sectional area, I is the second area moment, $\hat{W}(\hat{x},\hat{t})$ is the deflection, and $\hat{P}$ is the initial axial force in the beam. Parameters M, J, and L_L are, respectively, the mass, rotary inertia, and location of the lumped mass representing the comb-drives. $F(\hat{t})$ is the electrostatic excitation force. The subscripts $\hat{t}$ and $\hat{x}$ represent the derivation with respect to time and space, respectively. The prime also shows the spatial derivative. It is more appropriate to express Eq. (2) in dimensionless form, i.e.,

$$W_{tt}+\mu W_{tt}(\xi,t)\delta(x-\xi)-\mu\eta^2 W_{xtt}(\xi,t)\delta'(x-\xi)-2PW_{xx}+W_{xxxx}=\frac{1}{2r^2}(1-2r^2P)\left[W_{xx}\int_0^1 W_x^2\,\mathrm{d}x\right]+f\delta(x-\xi), \quad (3)$$

where

$$W=\frac{\hat{W}}{L},\quad t=\frac{\hat{t}}{L^2}\sqrt{\frac{EI}{\rho A}},$$

$$x=\frac{\hat{x}}{L},\quad P=\frac{\hat{P}L^2}{2EI},$$

$$\xi=\frac{L_L}{L},\quad \mu=\frac{M}{\rho AL},$$

$$r=\sqrt{\frac{I}{AL^2}},\quad \eta=\sqrt{\frac{J}{\mu\rho AL^3}},$$

$$f=\frac{FL^3}{EI}.$$

The deflection of the resonant beam can be expanded using the assumed modes method, i.e.,

$$W(x,t)=r^k\sum_{m=1}^{\infty}u_m(t)Y_m(x), \quad (4)$$

where k is an arbitrary real number larger than one [15]. $Y_m(x)$ and $u_m(t)$ are the m th normal mode and the m th generalized coordinate, respectively. The mode Y_m is the solution of spatial differential equation of the corresponding linear model [19], i.e.,

$$\omega_m^2[Y_m(x)+\mu Y_m(\xi)\delta(x-\xi)-\mu\eta^2 Y'_m(\xi)\delta'(x-\xi)]=Y_m^{(iv)}(x)-2PY''_m(x), \quad (5)$$

where ω_m is the m th dimensionless natural frequency. It is defined in terms of the m th physical natural frequency, $\hat{\omega}_m$, as

$$\omega_m=\hat{\omega}_m L^2\sqrt{\frac{\rho A}{EI}}. \quad (6)$$

Two distinct mode shapes Y_m and Y_n must satisfy the generalized orthogonality condition (see Refs. [19,20]), which can be expressed in dimensionless form as

$$\int_0^1 Y_m(x)Y_n(x)\,\mathrm{d}x+\mu Y_m(\xi)Y_n(\xi)+\mu\eta^2 Y'_m(\xi)Y'_n(\xi)=0 \quad \text{if } m\neq n. \quad (7)$$

Moreover, mode shapes can be made orthonormal; hence, for the case $m=n$,

$$\int_0^1 Y_m^2\,\mathrm{d}x+\mu Y_m^2(\xi)+\mu\eta^2 Y'^2_m(\xi)=1. \quad (8)$$

By substituting Eq. (4) into Eq. (3), one can show that

$$r^k\left\{\sum_{m=1}^{\infty}\ddot{u}_m[Y_m(x)+\mu Y_m(\xi)\delta(x-\xi)-\mu\eta^2 Y'_m(\xi)\delta'(x-\xi)]+\sum_{m=1}^{\infty}u_m[-2PY''_m(x)+Y_m^{(iv)}(x)]\right\}$$
$$=\frac{r^{3k-2}}{2}(1-2r^2P)\left[\left(\sum_{m=1}^{\infty}u_mY''_m\right)\int_0^1\left(\sum_{p=1}^{\infty}u_pY'_p\right)\left(\sum_{q=1}^{\infty}u_qY'_q\right)\mathrm{d}x\right]+f\delta(x-\xi). \quad (9)$$

Eq. (9) can be simplified as

$$\sum_{m=1}^{\infty}(\ddot{u}_m+\omega_m^2u_m)[Y_m(x)+\mu Y_m(\xi)\delta(x-\xi)-\mu\eta^2 Y'_m(\xi)\delta'(x-\xi)]$$
$$=\frac{r^{2(k-1)}}{2}(1-2r^2P)\left[\left(\sum_{m=1}^{\infty}u_mY''_m\right)\left(\sum_{p=1}^{\infty}\sum_{q=1}^{\infty}u_pu_q\int_0^1 Y'_pY'_q\,\mathrm{d}x\right)\right]+f\delta(x-\xi). \quad (10)$$

By multiplying Eq. (10) by Y_n, integrating over the range of x, i.e., $[0,1]$; and using Eqs. (7) and (8) as well as the definitions of Dirac's delta function, $\delta(x-\xi)$, and the doublet, $\delta'(x-\xi)$, Eq. (10) can be rewritten as

$$\ddot{u}_n+\omega_n^2 u_n=\frac{r^{2(k-1)}}{2}(1-2r^2P)\left[\left(\sum_{m=1}^{\infty}u_m\int_0^1 Y_m''\ Y_n\,\mathrm{d}x\right)\times\left(\sum_{p=1}^{\infty}\sum_{q=1}^{\infty}u_pu_q\int_0^1 Y_p'\ Y_q'\ \mathrm{d}x\right)\right]+\int_0^1 fY_n\delta(x-\xi)\,\mathrm{d}x. \tag{11}$$

Using integration by parts, one can show that

$$\int_0^1 Y_m''\ Y_n\,\mathrm{d}x=Y_mY_n'\,|_0^1-\int_0^1 Y_m'\ Y_n'\ \mathrm{d}x=-\int_0^1 Y_m'\ Y_n'\ \mathrm{d}x. \tag{12}$$

Consequently, the term in the bracket at the right side of Eq. (11) can be expressed in terms of Γ_{mnpq}, which is defined as

$$\begin{aligned}\Gamma_{mnpq}&=\frac{1}{2}(1-2r^2P)\left(\int_0^1 Y_m''\ Y_n\,\mathrm{d}x\right)\left(\int_0^1 Y_p'\ Y_q'\ \mathrm{d}x\right)\\&=-\frac{1}{2}(1-2r^2P)\left(\int_0^1 Y_m'\ Y_n'\ \mathrm{d}x\right)\left(\int_0^1 Y_p'\ Y_q'\ \mathrm{d}x\right)\quad\text{(from Eq. (12))}.\end{aligned} \tag{13}$$

By inspecting Eq. (13), the following identity can be concluded:

$$\Gamma_{mnpq}=\Gamma_{nmpq}=\Gamma_{mnqp}=\Gamma_{pqmn}. \tag{14}$$

Furthermore, the definition of Dirac's delta function implied that

$$f_n=\int_0^1 fY_n\delta(x-\xi)\,\mathrm{d}x=fY_n(\xi). \tag{15}$$

Letting $\varepsilon=r^{2(k-1)}$, Eq. (11) can be rewritten in a compact form as

$$\ddot{u}_n+\omega_n^2u_n=\varepsilon\sum_{m=1}^{\infty}\sum_{p=1}^{\infty}\sum_{q=1}^{\infty}u_mu_pu_q\Gamma_{nmpq}+f_n\quad(n=1,2,3,\ldots). \tag{16}$$

For those cases with damping, Eq. (16) can be extended by adding the modal damping term, $-2\varepsilon\zeta_n\dot{u}_n$, to the right side of it, i.e.,

$$\ddot{u}_n+\omega_n^2u_n=\varepsilon\left[\sum_{m=1}^{\infty}\sum_{p=1}^{\infty}\sum_{q=1}^{\infty}u_mu_pu_q\Gamma_{nmpq}-2\zeta_n\dot{u}_n\right]+f_n\quad(n=1,2,3,\ldots) \tag{17}$$

2.1. Free vibration

The stretching of a resonant beam, due to a large deflection, can shift the frequencies at which the beam vibrates. The extent of frequency shift depends on the initial condition of the beam oscillation. This phenomenon can be investigated using the governing equation of motion, Eq. (17), for the special case of undamped free vibration, i.e., $\zeta_n=0$ and $f_n=0$, i.e.,

$$\ddot{u}_n+\omega_n^2u_n=\varepsilon\sum_{m=1}^{\infty}\sum_{p=1}^{\infty}\sum_{q=1}^{\infty}u_mu_pu_q\Gamma_{nmpq}. \tag{18}$$

Application of the method of multiple scales implies that u_n can be expanded in the form of a power series in ε:

$$u_n=u_{n0}+\varepsilon u_{n1}+O(\varepsilon^2). \tag{19}$$

Time scales are defined as

$$T_0=t \tag{20}$$

and

$$T_1=\varepsilon t, \tag{21}$$

where T_0 and T_1 are called *fast time* and *slow time*, respectively. The operators representing the differentiation with respect to the time scales are defined as

$$D_0=\frac{\partial}{\partial T_0} \tag{22}$$

and

$$D_1=\frac{\partial}{\partial T_1}. \tag{23}$$

Consequently,

$$\frac{\mathrm{d}}{\mathrm{d}t}=D_0+\varepsilon D_1, \tag{24}$$

$$\frac{d^2}{dt^2} = D_0^2 + 2\varepsilon D_0 D_1. \tag{25}$$

Substituting Eqs. (19) and (25) into Eq. (18), one can show that

$$(D_0^2 + 2\varepsilon D_0 D_1)(u_{n0} + \varepsilon u_{n1}) + \omega_n^2(u_{n0} + \varepsilon u_{n1}) = \varepsilon \sum_{m,p,q=1}^{\infty} u_{m0}u_{p0}u_{q0}\Gamma_{nmpq}. \tag{26}$$

Collecting powers of ε yields a set of two differential equations for every mode n:

Order ε^0:

$$D_0^2 u_{n0} + \omega_n^2 u_{n0} = 0. \tag{27}$$

Order ε^1:

$$D_0^2 u_{n1} + \omega_n^2 u_{n1} = -2D_0 D_1 u_{n0} + \sum_{m,p,q=1}^{\infty} u_{m0}u_{p0}u_{q0}\Gamma_{nmpq}. \tag{28}$$

The solution of Eq. (27) is

$$u_{n0} = A_n(T_1)\exp(i\omega_n T_0) + cc, \tag{29}$$

where the amplitude A_n is a complex function of slow time, and cc represents the complex conjugates of the preceding terms. Substituting Eq. (29) into Eq. (28), one obtains

$$\begin{aligned} D_0^2 u_{n1} + \omega_n^2 u_{n1} = {} & -2i\omega_n D_1 A_n \exp(i\omega_n T_0) \\ & + \sum_{m,p,q=1}^{\infty} \Gamma_{nmpq}\{A_m A_p A_q \exp[i(\omega_m + \omega_p + \omega_q)T_0] + \overline{A}_m A_p A_q \exp[i(-\omega_m + \omega_p + \omega_q)T_0] \\ & + A_m \overline{A}_p A_q \exp[i(\omega_m - \omega_p + \omega_q)T_0] + A_m A_p \overline{A}_q \exp[i(\omega_m + \omega_p - \omega_q)T_0]\} + cc. \end{aligned} \tag{30}$$

The bar in this equation represents the complex conjugate of its corresponding parameter. The secular terms in Eq. (30) must be set to zero to ensure that the particular solution of u_{n1} is bounded. Those conditions resulting in secular terms are listed below:

$$\omega_m = \omega_n \text{ and } \omega_p = \omega_q \neq \omega_n \Rightarrow m = n, p = q \neq n \quad (2 \times p \text{ terms}),$$

$$\omega_p = \omega_n \text{ and } \omega_m = \omega_q \neq \omega_n \Rightarrow p = n, m = q \neq n \quad (2 \times m \text{ terms}),$$

$$\omega_q = \omega_n \text{ and } \omega_m = \omega_p \neq \omega_n \Rightarrow q = n, m = p \neq n \quad (2 \times m \text{ terms})$$

and

$$\omega_m = \omega_p = \omega_q = \omega_n \Rightarrow m = p = q = n \quad (3 \text{ terms}).$$

Considering Eq. (14), the above condition can be satisfied if

$$-2i\omega_n A_n' + \sum_{\substack{m=1 \\ m\neq n}}^{\infty} A_n A_m \overline{A}_m (4\Gamma_{nmnm} + 2\Gamma_{nnmm}) + 3A_n^2 \overline{A}_n \Gamma_{nnnn} = 0. \tag{31}$$

Noting that A_n is a complex function of the slow time, it can be expressed in polar form, in which the modulus and argument are functions of the slow time, i.e.,

$$A_n(T_1) = \tfrac{1}{2}a_n(T_1)\exp[i\beta_n(T_1)]. \tag{32}$$

Therefore, the differentiation of A_n with respect to T_1 can be expressed as

$$A_n'(T_1) = \tfrac{1}{2}a_n' \exp(i\beta_n) + \tfrac{1}{2}ia_n\beta_n' \exp(i\beta_n). \tag{33}$$

Substituting Eqs. (32) and (33) into Eq. (31), one can show that

$$-2i\omega_n\left[\frac{1}{2}a_n' \exp(i\beta_n) + \frac{1}{2}ia_n\beta_n' \exp(i\beta_n)\right] + \frac{1}{2}a_n \exp(i\beta_n) \sum_{\substack{m=1 \\ m\neq n}}^{\infty} \frac{1}{4}a_m^2(4\Gamma_{nmnm} + 2\Gamma_{nnmm}) + \frac{3}{8}a_n^3 \exp(i\beta_n)\Gamma_{nnnn} = 0. \tag{34}$$

Canceling out the exponential terms, collecting the real and imaginary terms, and then setting them to zero, Eq. (34) leads to

$$\omega_n a_n' = 0 \tag{35}$$

and

$$\omega_n a_n \beta_n' + \frac{1}{2}a_n \sum_{\substack{m=1 \\ m\neq n}}^{\infty} a_m^2\left(\Gamma_{nmnm} + \frac{1}{2}\Gamma_{nnmm}\right) + \frac{3}{8}a_n^3\Gamma_{nnnn} = 0. \tag{36}$$

ω_n is nonzero; hence, Eq. (35), implies that $a_n' = 0$. Therefore, $a_n = a_{n0} = \text{const}$. Eq. (36) can be solved for β_n' :

$$\beta_n' = -\frac{1}{\omega_n}\left[\frac{1}{2}\sum_{\substack{m=1\\m\neq n}}^{\infty} a_{m0}^2\left(\Gamma_{nmnm}+\frac{1}{2}\Gamma_{nnmm}\right)+\frac{3}{8}a_{n0}^2\Gamma_{nnnn}\right]. \tag{37}$$

The right side of Eq. (37) is constant; hence, this equation can be easily integrated with respect to T_1, i.e.,

$$\beta_n = -\frac{\varepsilon T_0}{\omega_n}\left[\frac{1}{2}\sum_{\substack{m=1\\m\neq n}}^{\infty} a_{m0}^2\left(\Gamma_{nmnm}+\frac{1}{2}\Gamma_{nnmm}\right)+\frac{3}{8}a_{n0}^2\Gamma_{nnnn}\right]+\beta_{n0}, \tag{38}$$

where T_1 is replaced by its equivalent expression εT_0. Substituting for a_n and β_n from the above equations into Eq. (32) and then Eq. (29), u_{n0} can be expressed as

$$\begin{aligned} u_{n0} &= \frac{1}{2}a_{n0}\exp[\mathrm{i}(\omega_n T_0+\beta_n)]+\mathrm{cc}\\ &= \frac{1}{2}a_{n0}\exp\left\{\mathrm{i}\left[\omega_n-\frac{\varepsilon}{\omega_n}\left(\frac{1}{2}\sum_{\substack{m=1\\m\neq n}}^{\infty} a_{m0}^2\left(\Gamma_{nmnm}+\frac{1}{2}\Gamma_{nnmm}\right)+\frac{3}{8}a_{n0}^2\Gamma_{nnnn}\right)\right]T_0+\mathrm{i}\beta_{n0}\right\}+\mathrm{cc}. \end{aligned} \tag{39}$$

The nonlinear resonance frequency can be found by inspecting the coefficient of T_0 in the argument of u_{n0} in Eq. (39), yielding

$$\omega_{n,\mathrm{nonlinear}} = \omega_n - \frac{\varepsilon}{\omega_n}\left[\frac{1}{2}\sum_{\substack{m=1\\m\neq n}}^{\infty} a_{m0}^2\left(\Gamma_{nmnm}+\frac{1}{2}\Gamma_{nnmm}\right)+\frac{3}{8}a_{n0}^2\Gamma_{nnnn}\right]. \tag{40}$$

2.2. Primary resonance

In most cases, resonators operate in the forced vibration mode. When the frequency of excitation is close to one of the natural frequencies of a resonator, primary resonance occurs. The linear vibration theory states that the resonance frequency is robust and independent of excitation. In addition, for very small damping ratios, the amplitude of vibration becomes extremely large, if not infinite. In contrast, as will be shown later, nonlinear analysis indicates that if the excitation, damping, and nonlinear restoring forces are of the same order, the resonance frequency will be a function of the frequency of excitation, and the amplitude of vibration will be bounded. For the primary resonance condition, the excitation force is assumed to be of the following form:

$$f = 2\varepsilon f_0\cos(\Omega t), \tag{41}$$

where Ω is the excitation frequency. The force amplitude is scales by ε to satisfy the primary resonance condition. Using Eq. (15), f_n can be expressed as

$$f_n = fY_n(\xi) = 2\varepsilon f_0 Y_n(\xi)\cos(\Omega t). \tag{42}$$

For the case of the excitation frequency being close to the fundamental natural frequency, Ω can be expressed as

$$\Omega = \omega_1 + \varepsilon\sigma_1, \tag{43}$$

where σ_1 indicates the difference between the excitation frequency and the fundamental natural frequency of the resonator. Substituting Eq. (42) into Eq. (17), the governing equation of motion can be reformulated as

$$\ddot{u}_n + \omega_n^2 u_n = \varepsilon\left[\sum_{m,p,q=1}^{\infty} u_m u_p u_q \Gamma_{nmpq} - 2\zeta_n\dot{u}_n\right] + 2\varepsilon f_0 Y_n(\xi)\cos(\Omega t). \tag{44}$$

By a similar approach presented in Section 2.1, and using Eqs. (18)–(25), (44) can be transformed into

$$\begin{aligned} (D_0^2+2\varepsilon D_0 D_1)(u_{n0}+\varepsilon u_{n1})+\omega_n^2(u_{n0}+\varepsilon u_{n1}) &= \varepsilon\left[\sum_{m,p,q=1}^{\infty} u_{m0}u_{p0}u_{q0}\Gamma_{nmpq} - 2\zeta_n(D_0+\varepsilon D_1)(u_{n0}+\varepsilon u_{n1})\right]\\ &\quad + 2\varepsilon f_0 Y_n(\xi)\cos(\Omega t). \end{aligned} \tag{45}$$

Collecting the powers of ε yields a set of two differential equations for each mode n:

Order ε^0:

$$D_0^2 u_{n0} + \omega_n^2 u_{n0} = 0. \tag{46}$$

Order ε^1:

$$D_0^2 u_{n1} + \omega_n^2 u_{n1} = -2D_0 D_1 u_{n0} - 2\zeta_n D_0 u_{n0} + \sum_{m,p,q=1}^{\infty} u_{m0}u_{p0}u_{q0}\Gamma_{nmpq} + 2f_0 Y_n(\xi)\cos(\Omega t). \tag{47}$$

As shown in Section 2.1, Eq. (46) has a solution of the form of Eq. (32). Eq. (42) can be expressed in polar form, i.e.,

$$f_n = \varepsilon f_0 Y_n(\xi)\exp(\mathrm{i}\Omega t) + \mathrm{cc}. \tag{48}$$

Substituting Eqs. (32) and (48) into Eq. (47), leads to

$$\begin{aligned} D_0^2 u_{n1} + \omega_n^2 u_{n1} = {} & -2\mathrm{i}\omega_n D_1 A_n \exp(\mathrm{i}\omega_n T_0) - 2\mathrm{i}\zeta_n \omega_n A_n \exp(\mathrm{i}\omega_n T_0) + f_0 Y_n(\xi)\exp(\mathrm{i}\Omega T_0) \\ & + \sum_{m,p,q=1}^{\infty} \Gamma_{nmpq}\{A_m A_p A_q \exp[\mathrm{i}(\omega_m + \omega_p + \omega_q)T_0] + \overline{A}_m A_p A_q \exp[\mathrm{i}(-\omega_m + \omega_p + \omega_q)T_0] \\ & + A_m \overline{A}_p A_q \exp[\mathrm{i}(\omega_m - \omega_p + \omega_q)T_0] + A_m A_p \overline{A}_q \exp[\mathrm{i}(\omega_m + \omega_p - \omega_q)T_0]\} + \mathrm{cc}. \end{aligned} \tag{49}$$

Seeking bounded solutions when t approaches to infinity, the secular terms in Eq. (49) must be eliminated. However, whether a particular term is secular or not, depends on higher natural frequencies of the resonator. In general, the ratio of the second to first natural frequency depends on the design of the resonant beam, particularly, on the mass ratio, rotary inertia, location of comb-drive, and the initial axial force in the beam. When the frequency ratio is close to three, the set of secular terms differs from those of cases in which this ratio is any other number. The special case of $\omega_2 \approx 3\omega_1$ is one of those several cases resulting in a phenomenon known as the *internal resonance*, which will be investigated later.

2.2.1. Primary resonance with no internal resonance

When $\omega_2 \not\approx 3\omega_1$, the secular terms in Eq. (49) that are associated with the summation operator term can be listed as follows:

$$\omega_m = \omega_n \text{ and } \omega_p = \omega_q \neq \omega_n \;\Rightarrow\; m = n, p = q \neq n \quad (2 \times p \text{ terms}),$$

$$\omega_p = \omega_n \text{ and } \omega_m = \omega_q \neq \omega_n \;\Rightarrow\; p = n, m = q \neq n \quad (2 \times m \text{ terms}),$$

$$\omega_q = \omega_n \text{ and } \omega_m = \omega_p \neq \omega_n \;\Rightarrow\; q = n, m = p \neq n \quad (2 \times m \text{ terms})$$

and

$$\omega_m = \omega_p = \omega_q = \omega_n \;\Rightarrow\; m = p = q = n \quad (3 \text{ terms}).$$

Consequently, for $n = 1$, the condition that eliminates the secular terms from Eq. (49) can be expressed as

$$-2\mathrm{i}\omega_1(A_1' + \zeta_1 A_1) + f_0 Y_1(\xi)\exp(\mathrm{i}\sigma_1 T_1) + A_1 \sum_{m=2}^{\infty} A_m \overline{A}_m (4\Gamma_{1m1m} + 2\Gamma_{11mm}) + 3A_1^2 \overline{A}_1 \Gamma_{1111} = 0. \tag{50}$$

Similarly, for $n \geq 2$, the following condition cancels out the unbounded solutions:

$$-2\mathrm{i}\omega_n(A_n' + \zeta_n A_n) + A_n \sum_{\substack{m=1 \\ m\neq n}}^{\infty} A_m \overline{A}_m (4\Gamma_{nmnm} + 2\Gamma_{nnmm}) + 3A_n^2 \overline{A}_n \Gamma_{nnnn} = 0. \tag{51}$$

By substituting Eqs. (32) and (33) into Eqs. (50) and (51), one obtains for $n = 1$:

$$-2\mathrm{i}\omega_1 \times \frac{1}{2}(a_1' + \mathrm{i}a_1\beta_1' + \zeta_1 a_1) + f_0 Y_1(\xi)\exp[i(\sigma_1 T_1 - \beta_1)] + \frac{1}{2}a_1 \sum_{m=2}^{\infty} \frac{1}{4} a_m^2 (4\Gamma_{1m1m} + 2\Gamma_{11mm}) + \frac{3}{8}a_1^3 \Gamma_{1111} = 0, \tag{52}$$

and for $n \geq 2$:

$$-2\mathrm{i}\omega_n \times \frac{1}{2}(a_n' + \mathrm{i}a_n\beta_n' + \zeta_n a_n) + \frac{1}{2}a_n \sum_{\substack{m=1 \\ m\neq n}}^{\infty} \frac{1}{4} a_m^2 (4\Gamma_{nmnm} + 2\Gamma_{nnmm}) + \frac{3}{8}a_n^3 \Gamma_{nnnn} = 0. \tag{53}$$

By collecting the real and imaginary terms, two equations can be derived from Eq. (52), i.e.,

$$-\omega_1(a_1' + \zeta_1 a_1) + f_0 Y_1(\xi)\sin(\sigma_1 T_1 - \beta_1) = 0 \tag{54}$$

and

$$\omega_1 a_1 \beta_1' + f_0 Y_1(\xi)\cos(\sigma_1 T_1 - \beta_1) + \frac{1}{2}a_1 \sum_{m=2}^{\infty} a_m^2 \left(\Gamma_{1m1m} + \frac{1}{2}\Gamma_{11mm}\right) + \frac{3}{8}a_1^3 \Gamma_{1111} = 0. \tag{55}$$

Similarly, Eq. (53) results in two equations:

$$-\omega_n(a_n' + \zeta_n a_n) = 0 \tag{56}$$

and

$$\omega_n a_n \beta_n' + \frac{1}{2}a_n \sum_{\substack{m=1 \\ m\neq n}}^{\infty} a_m^2 \left(\Gamma_{nmnm} + \frac{1}{2}\Gamma_{nnmm}\right) + \frac{3}{8}a_n^3 \Gamma_{nnnn} = 0. \tag{57}$$

Seeking a steady-state condition implies that

$$a_1' = a_n' = 0 \tag{58}$$

and

$$\sigma_1 T_1 - \beta_1 = \text{const.} \tag{59}$$

By substituting Eq. (58) into Eq. (56), one concludes that $a_n = 0$ ($n \geq 2$). Moreover, by differentiating Eq. (59) with respect to T_1, one obtains $\beta_1' = \sigma_1$. Letting $\gamma_1 = \sigma_1 T_1 - \beta_1$, Eqs. (54) and (55) can be simplified as

$$\begin{cases} \zeta_1 \omega_1 a_1 = f_0 Y_1(\xi) \sin\gamma_1, \\ \omega_1 a_1 \sigma_1 + f_0 Y_1(\xi) \cos\gamma_1 + \dfrac{3}{8} a_1^3 \Gamma_{1111} = 0, \end{cases} \tag{60}$$

from which, a_1 and γ_1 can be found as functions of σ_1.

2.2.2. Primary resonance with internal resonance

As mentioned in Section 2.2, when the second natural frequency is approximately three times of the first natural frequency, i.e., $\omega_2 \approx 3\omega_1$ and the excitation frequency is close to the first natural frequency, i.e., $\Omega \approx \omega_1$, internal resonance occurs, i.e., the amplitude of the second mode of vibration shows resonance behavior. These conditions can be stated mathematically as follows:

$$\omega_2 = 3\omega_1 + \varepsilon\sigma_1 \tag{61}$$

and

$$\Omega = \omega_1 + \varepsilon\sigma_2. \tag{62}$$

Using Eqs. (61) and (62) the secular terms in Eq. (49) that are associated with the summation operator term can be listed as

$$\omega_m = \omega_n \text{ and } \omega_p = \omega_q \neq \omega_n \;\Rightarrow\; m = n, p = q \neq n \quad (2 \times p \text{ terms}),$$

$$\omega_p = \omega_n \text{ and } \omega_m = \omega_q \neq \omega_n \;\Rightarrow\; p = n, m = q \neq n \quad (2 \times m \text{ terms}),$$

$$\omega_q = \omega_n \text{ and } \omega_m = \omega_p \neq \omega_n \;\Rightarrow\; q = n, m = p \neq n \quad (2 \times m \text{ terms})$$

and

$$\omega_m = \omega_p = \omega_q = \omega_n \;\Rightarrow\; m = p = q = n \quad (3 \text{ terms}).$$

Hence, the equations that eliminate unbounded terms from Eq. (49) can be derived as

For $n = 1$:

$$-2\mathrm{i}\omega_1(A_1' + \zeta_1 A_1) + f_0 Y_1(\xi)\exp(\mathrm{i}\sigma_2 T_1) + A_1 \sum_{m=2}^{\infty} A_m \overline{A}_m (4\Gamma_{1m1m} + 2\Gamma_{11mm}) + 3A_1^2 \overline{A}_1 \Gamma_{1111} + 3A_2 \overline{A}_1^2 \Gamma_{2111} \exp(\mathrm{i}\sigma_1 T_1) = 0. \tag{63}$$

For $n = 2$:

$$-2\mathrm{i}\omega_2(A_2' + \zeta_2 A_2) + A_2 \sum_{\substack{m=1 \\ m\neq 2}}^{\infty} A_m \overline{A}_m (4\Gamma_{2m2m} + 2\Gamma_{22mm}) + 3A_2^2 \overline{A}_2 \Gamma_{2222} + A_1^3 \Gamma_{2111} \exp(-\mathrm{i}\sigma_1 T_1) = 0. \tag{64}$$

For $n \geq 3$:

$$-2\mathrm{i}\omega_n(A_n' + \zeta_n A_n) + A_n \sum_{\substack{m=1 \\ m\neq n}}^{\infty} A_m \overline{A}_m (4\Gamma_{nmnm} + 2\Gamma_{nnmm}) + 3A_n^2 \overline{A}_n \Gamma_{nnnn} = 0. \tag{65}$$

Letting $\gamma_1 = \sigma_1 T_1 - 3\beta_1 + \beta_2$ and $\gamma_2 = \sigma_2 T_1 - \beta_1$, and then substituting Eqs. (32) and (33) into Eqs. (63)–(65), one obtains

For $n = 1$:

$$-2\mathrm{i}\omega_1 \times \frac{1}{2}(a_1' + \mathrm{i}a_1\beta_1' + \zeta_1 a_1) + f_0 Y_1(\xi)\exp(\mathrm{i}\gamma_2) + \frac{1}{8} a_1 \sum_{m=2}^{\infty} a_m^2 (4\Gamma_{1m1m} + 2\Gamma_{11mm}) + \frac{3}{8} a_1^3 \Gamma_{1111} + \frac{3}{8} a_1^2 a_2 \Gamma_{2111} \exp(\mathrm{i}\gamma_1) = 0. \tag{66}$$

For $n = 2$:

$$-2\mathrm{i}\omega_2 \times \frac{1}{2}(a_2' + \mathrm{i}a_2\beta_2' + \zeta_2 a_2) + \frac{1}{8} a_2 \sum_{\substack{m=1 \\ m\neq 2}}^{\infty} a_m^2 (4\Gamma_{2m2m} + 2\Gamma_{22mm}) + \frac{3}{8} a_2^3 \Gamma_{2222} + \frac{1}{8} a_1^3 \Gamma_{2111} \exp(-\mathrm{i}\gamma_1) = 0. \tag{67}$$

For $n \geq 3$:

$$-2\mathrm{i}\omega_n \times \frac{1}{2}(a_n' + \mathrm{i}a_n\beta_n' + \zeta_n a_n) + \frac{1}{8} a_n \sum_{\substack{m=1 \\ m\neq n}}^{\infty} a_m^2 (4\Gamma_{nmnm} + 2\Gamma_{nnmm}) + \frac{3}{8} a_n^3 \Gamma_{nnnn} = 0. \tag{68}$$

By collecting real and imaginary terms and setting them to zero, two equations can be derived from each equations above; therefore, from Eq. (68), one concludes that

$$a_n' + \zeta a_n = 0 \quad (n \geq 3). \tag{69}$$

For $n \geq 1$, $a_n' = 0$ due to imposing the steady-state condition. Therefore, from Eq. (69), $a_n = 0$ for $n \geq 3$. The two equations derived from Eq. (66) are

$$-\omega_1(a_1' + \zeta_1 a_1) + f_0 Y_1(\xi)\sin\gamma_2 + \tfrac{3}{8}a_1^2 a_2 \Gamma_{2111}\sin\gamma_1 = 0, \tag{70}$$

$$\omega_1 a_1 \beta_1' + f_0 Y_1(\xi)\cos\gamma_2 + \tfrac{3}{8}a_1^3\Gamma_{1111} + \tfrac{1}{8}a_1 a_2^2(4\Gamma_{1212} + 2\Gamma_{1122}) + \tfrac{3}{8}a_1^2 a_2 \Gamma_{2111}\cos\gamma_1 = 0. \tag{71}$$

Similarly, the two equations derived from Eq. (67) are

$$-\omega_2(a_2' + \zeta_2 a_2) - \tfrac{1}{8}a_1^3\Gamma_{2111}\sin\gamma_1 = 0, \tag{72}$$

$$\omega_2 a_2 \beta_2' + \tfrac{3}{8}a_2^3\Gamma_{2222} + \tfrac{1}{8}a_1^2 a_2(4\Gamma_{2121} + 2\Gamma_{2211}) + \tfrac{1}{8}a_1^3\Gamma_{2111}\cos\gamma_1 = 0. \tag{73}$$

The steady-state condition implies that $a_1' = a_2' = 0$ and $\gamma_1' = \gamma_2' = 0$; hence, $\beta_1' = \sigma_2$ and $\beta_2' = 3\sigma_2 - \sigma_1$. Therefore,

$$\begin{cases} -\omega_1\zeta_1 a_1 + f_0 Y_1(\xi)\sin\gamma_2 + \dfrac{3}{8}a_1^2 a_2 \Gamma_{2111}\sin\gamma_1 = 0, \\ \omega_1\sigma_1 a_1 + f_0 Y_1(\xi)\cos\gamma_2 + \dfrac{3}{8}a_1^3\Gamma_{1111} + \dfrac{1}{8}a_1 a_2^2(4\Gamma_{1212} + 2\Gamma_{1122}) + \dfrac{3}{8}a_1^2 a_2\Gamma_{2111}\cos\gamma_1 = 0, \\ \omega_2\zeta_2 a_2 + \dfrac{1}{8}a_1^3\Gamma_{2111}\sin\gamma_1 = 0, \\ \omega_2(3\sigma_2 - \sigma_1)a_2 + \dfrac{3}{8}a_2^3\Gamma_{2222} + \dfrac{1}{8}a_1^2 a_2(4\Gamma_{2121} + 2\Gamma_{2211}) + \dfrac{1}{8}a_1^3\Gamma_{2111}\cos\gamma_1 = 0. \end{cases} \tag{74}$$

Eq. (74) can be solved for a_1, a_2, γ_1, and γ_2 as functions of σ_1 and σ_2.

3. Results

In this section, the numerical results of the modeling are presented. First, the effect of the stretching of the beam on the free vibration of beam-mass systems is discussed. Then, the nonlinear primary resonance of some beam-lumped mass systems, in which the natural frequencies do not satisfy the condition for internal resonance, are presented. Finally, two cases in which internal resonance occur, are discussed in detail.

3.1. Free vibration

Eq. (40) provides the frequency of the free vibration of a beam-lumped mass system as a function of the linear natural frequency, initial axial force, and initial modal displacements, a_{m0}. In Fig. 4, the nonlinear frequency of vibration is plotted versus the initial modal displacement of the first mode, a_{10}, for different number of modes. It has been assumed that $\varepsilon = 0.01$, $\mu = 1$, $\eta = 1$, $\xi = 0.4$, and $P = 0$. The vertical axis of Fig. 4 is the initial amplitude of the first mode. To be more realistic, it is assumed that the amplitudes of higher modes are reduced by a factor of 10, i.e., $a_{20} = 0.1a_{10}$, $a_{30} = 0.1a_{20}$, and so on. Although the amplitudes of higher modes are reduced, this figure reveals that these modes have a significant effect on the frequency of free vibration of the system, and cannot be neglected as previous studies suggest [16,17,21–24].

Tables 1 and 2 present the first four natural frequencies and the nonlinear frequencies of the free vibration of six illustrative cases. The initial displacements are assumed equal to 10, i.e., $a_{m0} = 10$, which are practically very large displacements. The reason for choosing these large amplitudes is to achieve large differences between the linear and nonlinear natural frequencies, which enable us to investigate the effect of other parameters. The first three cases correspond to a single asymmetric resonator with tensile, compressive, and zero initial axial forces. The difference between the nonlinear free vibration frequency and the natural frequency at each mode indicates the influence of the stretching on the vibration frequency. These cases reveal that the difference between linear and nonlinear free vibration frequencies for a beam under compressive axial force is significantly greater than those of cases with zero or tensile axial force, even when the magnitude of the tensile axial force is several times larger than the compressive force. It must be noted that the maximum allowable compressive axial force is $P = -2\pi^2$, which is the theoretical buckling force [29]. This difference can be explained by noting that the stretching effect induces a tensile axial force, which will be superimposed to the initial axial force in the beam, and subsequently, will change the effective axial force. The higher sensitivity of a beam-lumped mass system under initial compressive axial force to the stretching is in agreement with earlier findings that suggest these systems, when used as force sensors, depict more sensitivity to the change of axial force [3].

Case 4 is a symmetric resonator which will be studied for the primary resonance later in this paper. This case can be compared with case 1, which is similar except in the mass location. It can be observed that the symmetric beam-lumped mass system shows higher sensitivity to the stretching at the first mode only, while the asymmetric system is more sensitive at higher modes. This can be referred to the different mode shapes of the system and their effects on the

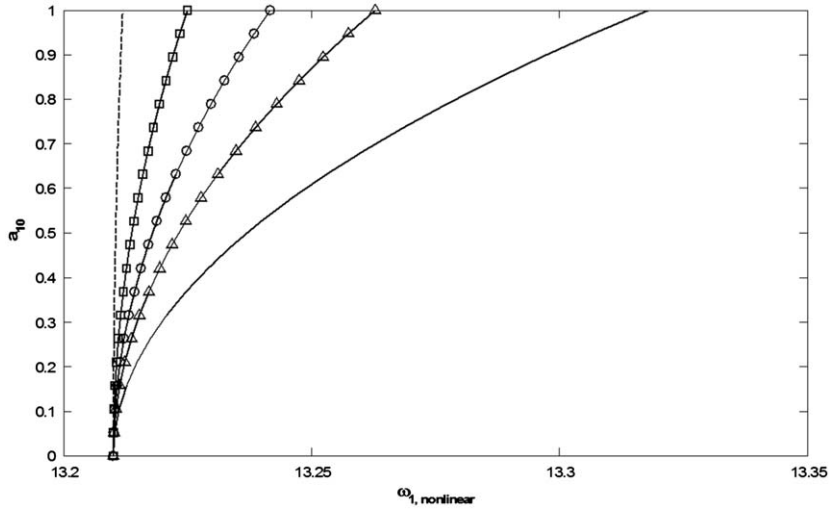

Fig. 4. The fundamental frequency of free vibration of a beam-lumped mass system with $\mu = 1$, $\eta = 1$, $\xi = 0.4$, and $P = 0$ as a function of the initial displacement for different number of included modes: first mode (dashed), first two modes (square-line), first three modes (circle-line), first four modes (triangle-line), and first five modes (solid).

Table 1
First and second nonlinear natural frequencies of vibration of a clamped–clamped beam with lumped mass.

Case no.	P	ξ	μ	η	ω_1	$\omega_{1,\text{nonlinear}}$	ω_2	$\omega_{2,\text{nonlinear}}$
1	0	0.25	1	1	23.21	42.80	42.79	102.09
2	100	0.25	1	1	38.03	46.79	81.23	104.12
3	−18	0.25	1	1	18.87	49.34	30.57	118.60
4	0	0.5	1	1	11.82	39.20	89.40	144.26
5	0	0.32	1	1.31	16.95	36.97	50.85	101.44
6	25	0.33	1	0.8	21.41	35.66	65.07	102.31

Table 2
Third and fourth nonlinear natural frequencies of vibration of a clamped–clamped beam with lumped mass.

Case no.	P	ξ	μ	η	ω_3	$\omega_{3,\text{nonlinear}}$	ω_4	$\omega_{4,\text{nonlinear}}$
1	0	0.25	1	1	111.96	190.70	217.20	315.78
2	100	0.25	1	1	170.60	211.27	287.42	347.26
3	−18	0.25	1	1	97.40	192.12	201.88	312.12
4	0	0.5	1	1	95.76	155.73	246.66	336.77
5	0	0.32	1	1.31	135.76	209.53	223.49	281.34
6	25	0.33	1	0.8	157.34	218.56	224.12	274.30

stretching. In cases 5 and 6, the ratio of the second to the first natural frequencies is close to 3. These cases will be investigated later in the internal resonance of beam-lumped mass systems.

3.2. Primary resonance, non-internal resonance

In this section, the results of the primary resonance of three beam-lumped mass systems will be presented for those cases not resulting in an internal resonance. For all cases, the amplitude of excitation is assumed to be $f_0 = 1$. Fig. 5 shows the frequency response amplitude of a symmetric beam-lumped mass system with $\xi = 0.5$, $\mu = 1$, $\eta = 1$, $\zeta = 0.01$ for various axial forces. It can be observed that the system with compressive axial force shows more sensitivity to the stretching in primary resonance. Moreover, the system with tensile axial force shows the least deviation from linear behavior. This observation is in agreement with that of free vibration study.

Fig. 6 shows the frequency response of three beam-lumped mass systems with different mass locations. As shown, the symmetric system depicts the largest response amplitude, while the response for $\xi = 0.2$ is the smallest one. This difference can be explained by noting that the amplitude of excitation is equal for all these cases, but the mode shape of a

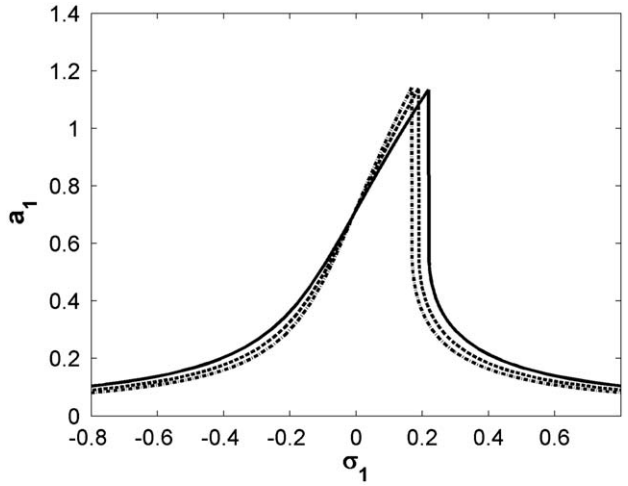

Fig. 5. The primary resonance of a symmetric beam-lumped mass system with $\mu = 1$, $\eta = 1$, $\xi = 0.5$, and $\zeta = 0.01$, for different axial forces, $P = -5$ (solid), $P = 0$ (dashed), and $P = 5$ (dashed-dotted).

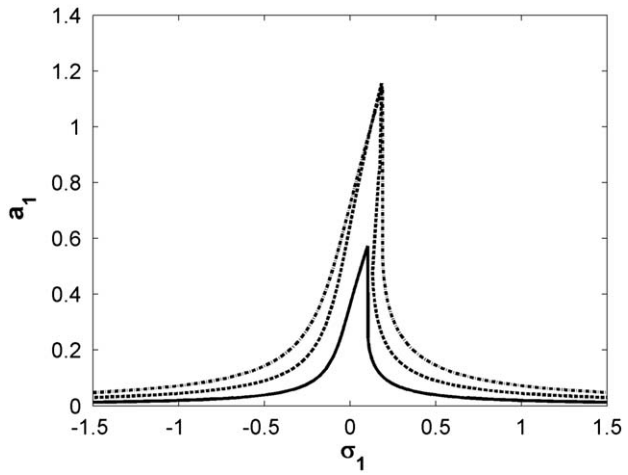

Fig. 6. The primary resonance of different beam-lumped mass systems with $\mu = 1$, $\eta = 1$, $P = 0$, and $\zeta = 0.01$, for different lumped mass locations, $\xi = 0.2$ (solid), $\xi = 0.3$ (dashed), and $\xi = 0.5$ (dashed-dotted).

symmetric system shows larger deflection at the point where excitation is applied. Therefore, it can be concluded that an asymmetric system is less prone to stretching effects.

The effect of rotary inertia on the nonlinear behavior of a beam-lumped mass system is shown in Fig. 7. As depicted, when the radius of gyration is zero, the amplitude of the response is less than those of cases with nonzero radii of gyration. This can be addressed by noting that the rotary inertia significantly changes the mode shape of vibration, and hence the effect of stretching.

The effect of damping ratio on the nonlinear response of a beam-lumped mass system can be found in Fig. 8. As expected, by increasing the damping ratio, the nonlinear response vanishes.

3.3. Primary resonance, internal resonance

In this section, the results of the internal resonance of beam-lumped mass systems will be presented for cases 5 and 6 in Tables 1 and 2. The ratio of the second to first natural frequencies of case 5 is 3.000005, which indicates that this resonator is prone to internal resonance. Fig. 9 shows the amplitude of the second mode, a_2, when the beam is excited at the first natural frequency. This figure is significant for showing a resonance peak at the second mode, while the excitation frequency is close to the resonance frequency of the first mode. It can be observed that the internal resonance occurs only for extremely small damping ratios, and even the damping ratio of $\zeta = 0.01$, which is practically small, diminishes the internal resonance. Although these small damping ratios are rarely observed in macro-systems, damping ratios of the order of 10^{-4} are common for micro-systems with very high quality factors. In addition, measuring very small amplitudes of

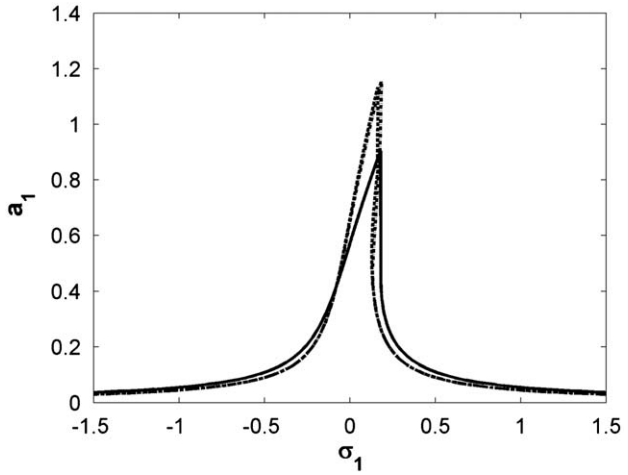

Fig. 7. The primary resonance of different beam-lumped mass systems with $\mu = 1$, $\xi = 0.3$, $P = 0$, and $\zeta = 0.01$, for different lumped mass radius of gyrations, $\eta = 0$ (solid), $\eta = 0.5$ (dashed), and $\eta = 1$ (dashed-dotted).

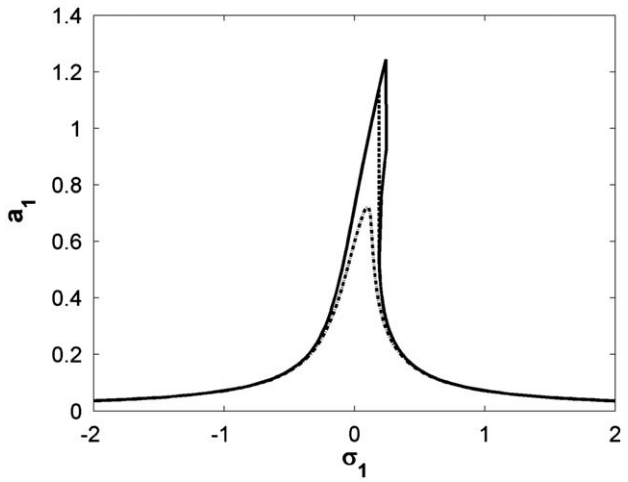

Fig. 8. The primary resonance of a symmetric beam-lumped mass system with $\mu = 1$, $\eta = 1$, $\xi = 0.5$, and $P = 0$, for different damping ratios, $\zeta = 0.005$ (solid), $\zeta = 0.01$ (dashed), and $\zeta = 0.1$ (dashed-dotted).

vibration with high resolution is practical, thanks to the development of Laser Doppler Velocimetry techniques. The response of the first mode at the internal resonance for the damping ratio of $\zeta = 0.001$ is shown in Fig. 10. Noting the vertical axis of this diagram, one concludes that the variations of a_1 are very small, though nonzero. For each damping ratio, the curve of a_1 is normalized by subtracting the minimum of the curve from itself, Fig. 11. This figure shows that by increasing the damping ratio, the variations of a_1 are decreased. The parameters γ_1 and γ_2, which are used for finding the phase of response are plotted in Figs. 12–14. It must be noted that Fig. 13 is similar to Fig. 10 in the sense that its variations are small. Moreover, the curves in Fig. 14 are normalized with a similar procedure as in Fig. 11.

The second to first frequency ratio of case 6 is 3.039575. Fig. 15 depicts the amplitude of the second mode of case 6 at internal resonance. Similar to Fig. 9, increasing the damping ratio decreases the effect of the nonlinearity. Moreover, by comparing the maximums of the curves in these two figures, one concludes that the nonlinear response in case 6, in which a tensile axial force is applied, is significantly less than that of case 5. The same conclusion can be drawn about the amplitude of the first mode, Fig. 16 versus Fig. 10, and its variation, Fig. 17 versus Fig. 11. This conclusion is in agreement with the findings of the free vibration investigation. The curves of γ_1 in Fig. 18, on the other hand, are very similar to those of Fig. 12, and show a 180° change in phase at resonance.

By comparing Fig. 19, in which γ_2 for the case of $\zeta = 0.001$ is plotted, with Fig. 13, one can confirm that the variation is reduced due to the tensile axial force. The normalized curves of γ_2 for different damping ratios are plotted in Fig. 20. It is noticeable that the variations in these curves are one order of magnitude smaller than those of Fig. 14.

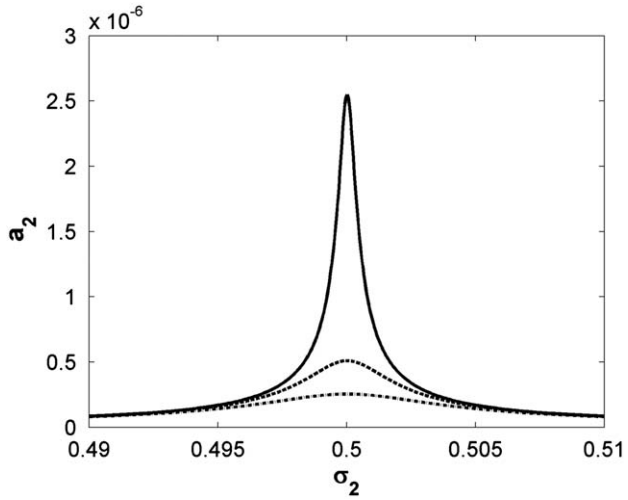

Fig. 9. The amplitude of the second mode, a_2, at the internal resonance of an asymmetric beam-lumped mass system with $\mu = 1$, $\eta = 1.31$, $\xi = 0.32$, and $P = 0$, for different damping ratios, $\zeta = 0.001$ (solid), $\zeta = 0.005$ (dashed), and $\zeta = 0.01$ (dashed-dotted).

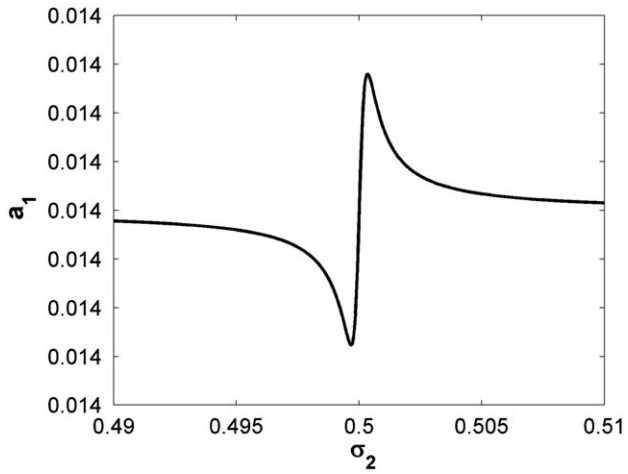

Fig. 10. The amplitude of the first mode, a_1, at the internal resonance of an asymmetric beam-lumped mass system with $\mu = 1$, $\eta = 1.31$, $\xi = 0.32$, $P = 0$, and $\zeta = 0.001$.

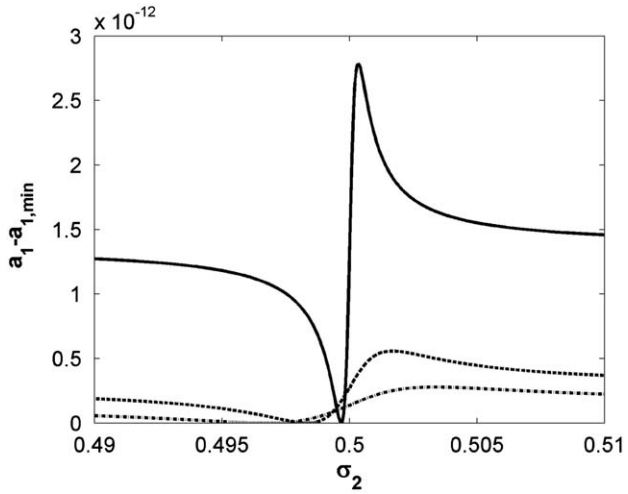

Fig. 11. The relative amplitude of the first mode, a_1, at the internal resonance of an asymmetric beam-lumped mass system with $\mu = 1$, $\eta = 1.31$, $\xi = 0.32$, and $P = 0$, for different damping ratios, $\zeta = 0.001$ (solid), $\zeta = 0.005$ (dashed), and $\zeta = 0.01$ (dashed-dotted).

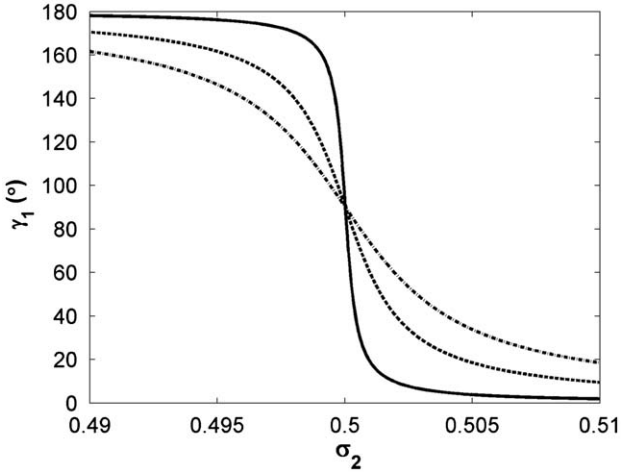

Fig. 12. The phase γ_1 at the internal resonance of an asymmetric beam-lumped mass system with $\mu = 1$, $\eta = 1.31$, $\xi = 0.32$, and $P = 0$, for different damping ratios, $\zeta = 0.001$ (solid), $\zeta = 0.005$ (dashed), and $\zeta = 0.01$ (dashed-dotted).

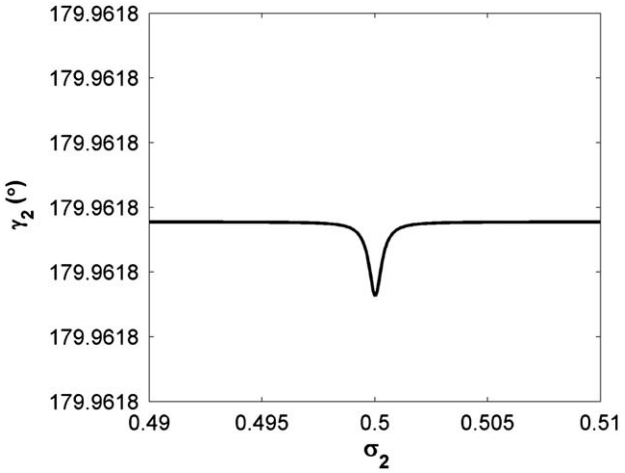

Fig. 13. The phase γ_2 at the internal resonance of an asymmetric beam-lumped mass system with $\mu = 1$, $\eta = 1.31$, $\xi = 0.32$, $P = 0$, and $\zeta = 0.001$.

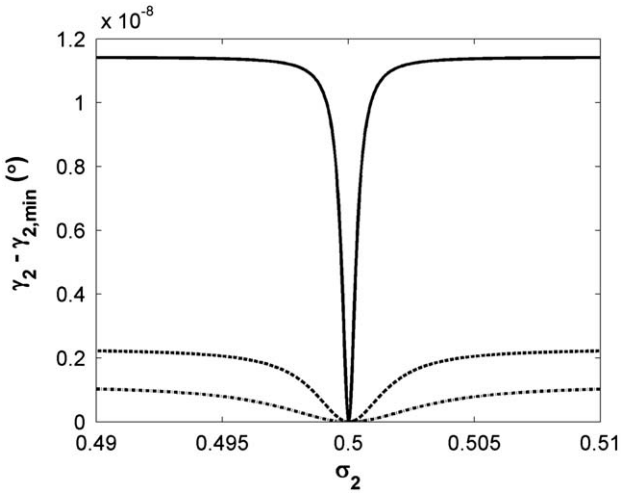

Fig. 14. The relative phase γ_2 at the internal resonance of an asymmetric beam-lumped mass system with $\mu = 1$, $\eta = 1.31$, $\xi = 0.32$, and $P = 0$, for different damping ratios, $\zeta = 0.001$ (solid), $\zeta = 0.005$ (dashed), and $\zeta = 0.01$ (dashed-dotted).

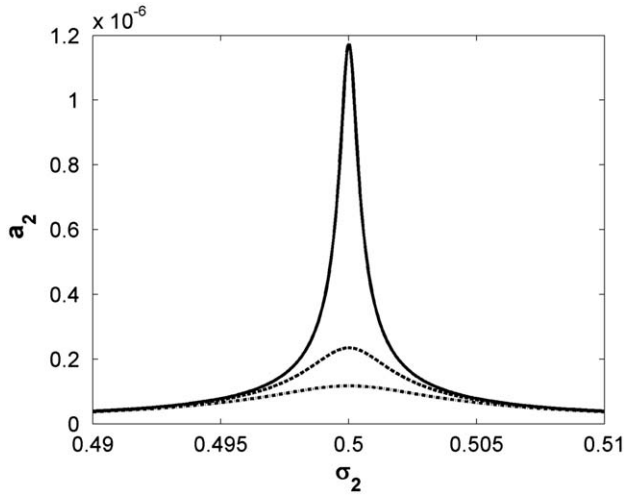

Fig. 15. The amplitude of the second mode, a_2, at the internal resonance of an asymmetric beam-lumped mass system with $\mu = 1$, $\eta = 0.8$, $\xi = 0.33$, and $P = 25$, for different damping ratios, $\zeta = 0.001$ (solid), $\zeta = 0.005$ (dashed), and $\zeta = 0.01$ (dashed-dotted).

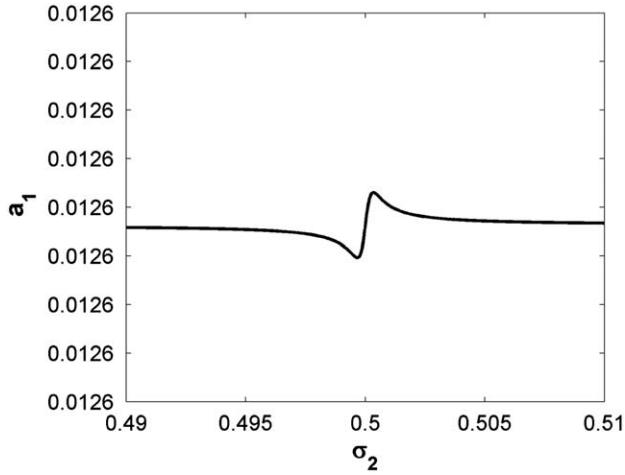

Fig. 16. The amplitude of the first mode, a_1, at the internal resonance of an asymmetric beam-lumped mass system with $\mu = 1$, $\eta = 0.8$, $\xi = 0.33$, and $P = 25$, and $\zeta = 0.001$.

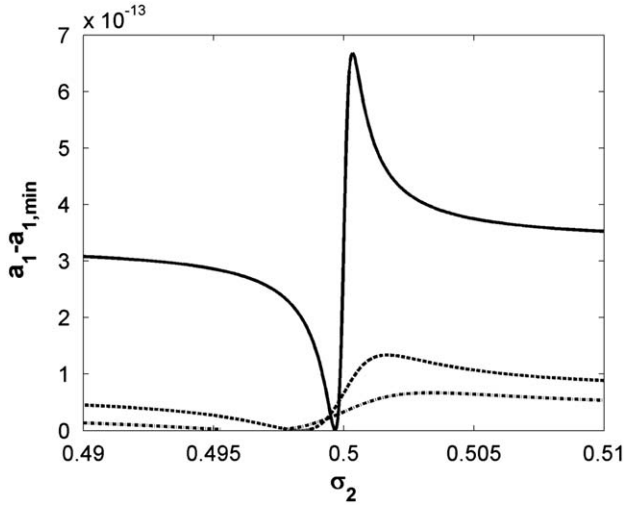

Fig. 17. The relative amplitude of the first mode, a_1, at the internal resonance of an asymmetric beam-lumped mass system with $\mu = 1$, $\eta = 0.8$, $\xi = 0.33$, and $P = 25$, for different damping ratios, $\zeta = 0.001$ (solid), $\zeta = 0.005$ (dashed), and $\zeta = 0.01$ (dashed-dotted).

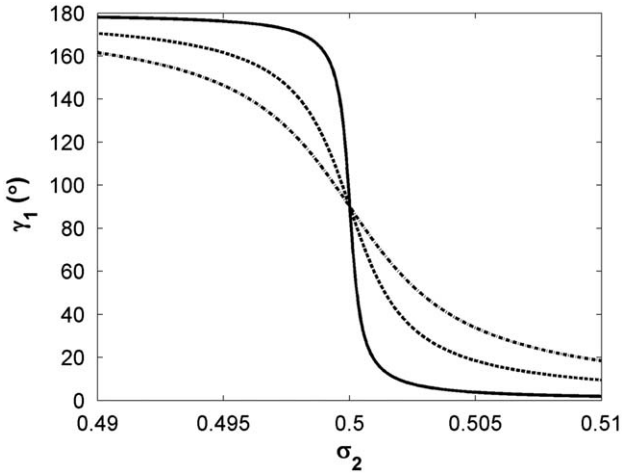

Fig. 18. The phase γ_1 at the internal resonance of an asymmetric beam-lumped mass system with $\mu = 1$, $\eta = 0.8$, $\xi = 0.33$, and $P = 25$, for different damping ratios, $\zeta = 0.001$ (solid), $\zeta = 0.005$ (dashed), and $\zeta = 0.01$ (dashed-dotted).

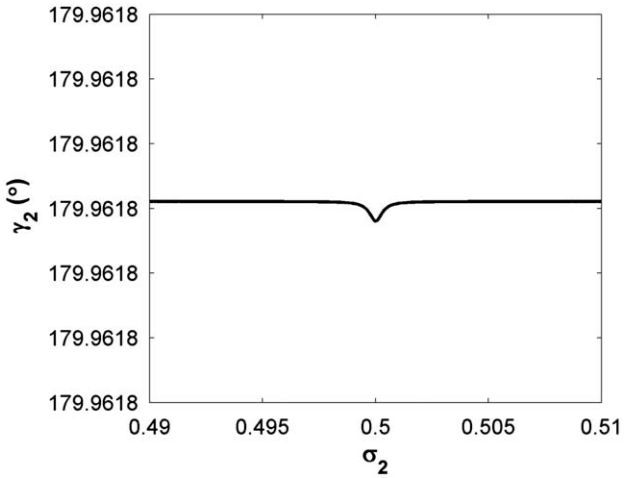

Fig. 19. The phase γ_2 at the internal resonance of an asymmetric beam-lumped mass system with $\mu = 1$, $\eta = 0.8$, $\xi = 0.33$, and $P = 25$, and $\zeta = 0.001$.

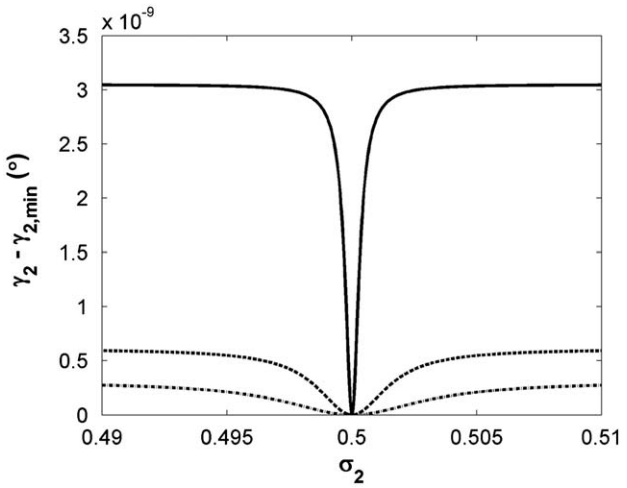

Fig. 20. The relative phase γ_2 at the internal resonance of an asymmetric beam-lumped mass system with $\mu = 1$, $\eta = 0.8$, $\xi = 0.33$, and $P = 25$, for different damping ratios, $\zeta = 0.001$ (solid), $\zeta = 0.005$ (dashed), and $\zeta = 0.01$ (dashed-dotted).

4. Conclusions

The dynamics of a micro-bridge with attached electrostatic comb-drives is studied in this paper. When the deflection of the micro-bridge is comparable with its size, the system shows nonlinear behavior. A thin beam model, which also takes into account the effects of the modal damping, and initial axial force in the beam as well as mass, location, and rotary inertia of the electrostatic comb-drives, is used to investigate free and forced nonlinear vibrations. For asymmetric resonators, i.e., resonators in which the electrostatic comb-drives are closer to either beam ends, certain combinations of the above parameters can be found that generate internal resonance between different modes. It is observed that a tensile initial axial force reduces the nonlinearity due to a large deflection, while a compressive axial force amplifies the nonlinearity. The results of this paper can be applied in the design of micromachined resonant sensors with enhanced sensitivity.

References

[1] N. Lobontiu, E. Garcia, *Mechanics of Microelectromechanical Systems*, Kluwer Academic, New York, 2005.
[2] P.A. Hassanpour, W.L. Cleghorn, J.K. Mills, E. Esmailzadeh, Exact solution of the oscillatory behavior under axial force of a beam with a concentrated mass within its interval, *Journal of Vibration and Control* 13 (12) (2007) 1723–1739.
[3] P.A. Hassanpour, W.L. Cleghorn, E. Esmailzadeh, J.K. Mills, Vibration analysis of micro-machined beam-type resonators, *Journal of Sound and Vibration* 308 (1–2) (2007) 287–301.
[4] P.A. Hassanpour, Design and Analysis of Micro-Electromechanical Resonant Structures, PhD Thesis, University of Toronto, Canada, 2008.
[5] K.L. Turner, S.A. Miller, P.G. Hartwell, N.C. MacDonald, S.H. Strogatz, S.G. Adams, Five parametric resonances in a microelectromechanical system, *Nature* 396 (6707) (1998) 149–152.
[6] B.K. Hammad, A.H. Nayfeh, E. Abdel-Rahman, A subharmonic resonance—based MEMS filter, *Proceedings of the ASME International Mechanical Engineering Congress and Exposition*, 2007, pp. 303–312.
[7] B.E. DeMartini, H.E. Butterfield, J. Moehlis, K.L. Turner, Chaos for a microelectromechanical oscillator governed by the nonlinear Mathieu equation, *Journal of Microelectromechanical Systems* 16 (6) (2007) 1314–1323.
[8] B.E. DeMartini, J.F. Rhoads, K.L. Turner, S.W. Shaw, J. Moehlis, Linear and nonlinear tuning of parametrically excited MEMS oscillators, *Journal of Microelectromechanical Systems* 16 (2) (2007) 310–318.
[9] A.H. Nayfeh, M.I. Younis, E.M. Abdel-Rahman, Dynamic analysis of MEMS resonators under primary-resonance excitation, *Proceedings of the ASME International Design Engineering Technical Conferences and Computers and Information in Engineering Conference*, Vol. 1, Pts A-C, pp. 397–404, 2005, *20th Biennial Conference on Mechanical Vibration and Noise*, Long Beach, CA, September 24–28, 2005.
[10] M.F. Yu, G.J. Wagner, R.S. Ruoff, M.J. Dyer, Realization of parametric resonances in a nanowire mechanical system with nanomanipulation inside a scanning electron microscope, *Physical Review B* 66 (7) (2002).
[11] W.H. Zhang, R. Baskaran, K.L. Turner, Effect of cubic nonlinearity on auto-parametrically amplified resonant MEMS mass sensor, *Sensors and Actuators A-Physical* 102 (1–2) (2002) 139–150.
[12] W.H. Zhang, R. Baskaran, K.L. Turner, Tuning the dynamic behavior of parametric resonance in a micromechanical oscillator, *Applied Physics Letters* 82 (1) (2003) 130–132.
[13] B.H. Bahreyni, C. Shafai, A resonant micromachined magnetic field sensor, *IEEE Sensors Journal* 7 (9–10) (2007) 1326–1334.
[14] B.H. Bahreyni, Design, Modeling, Simulation, and Testing of Resonant Micromachined Magnetic Field Sensors, PhD Thesis, University of Manitoba, Canada, 2006.
[15] A.H. Nayfeh, D.T. Mook, *Nonlinear Oscillations*, Wiley, New York, 1979.
[16] E. Ozkaya, M. Pakdemirli, H.R. Oz, Non-linear vibrations of a beam-mass system under different boundary conditions, *Journal of Sound and Vibration* 199 (3) (1997) 679–696.
[17] E. Ozkaya, M. Pakdemirli, H.R. Oz, Non-linear vibrations of a beam-mass system under different boundary conditions—reply, *Journal of Sound and Vibration* 207 (2) (1997) 286.
[18] K.H. Low, Comments on "non-linear vibrations of a beam-mass system under different boundary conditions", *Journal of Sound and Vibration* 207 (1997) 284–286.
[19] P.A. Hassanpour, E. Esmailzadeh, W.L. Cleghorn, J.K. Mills, Generalized orthogonality condition for beams with intermediate lumped masses subjected to axial force, *Journal of Vibration and Control*, in press, doi:10.1177/1077546309106526.
[20] D.I.M. Forehand, M.P. Cartmell, On the derivation of the equations of motion for a parametrically excited cantilever beam, *Journal of Sound and Vibration* 245 (1) (2001) 165–177.
[21] E. Ozkaya, M. Pakdemirli, Non-linear vibrations of a beam-mass system with both ends clamped, *Journal of Sound and Vibration* 221 (3) (1999) 491–503.
[22] E. Ozkaya, Non-linear transverse vibrations of a simply supported beam carrying concentrated masses, *Journal of Sound and Vibration* 257 (3) (2002) 413–424.
[23] M. Pakdemirli, H. Boyaci, Non-linear vibrations of a simple–simple beam with a non-ideal support in between, *Journal of Sound and Vibration* 268 (2) (2003) 331–341.
[24] E. Ozkaya, A. Tekin, Non linear vibrations of stepped beam system under different boundary conditions, *Structural Engineering and Mechanics* 27 (3) (2007) 333–345.
[25] A. Ramezani, A. Alasty, J. Akbari, Effects of rotary inertia and shear deformation on nonlinear free vibration of microbeams, *Journal of Vibration and Acoustics—Transactions of the ASME* 128 (5) (2006) 611–615.
[26] A. Vyas, D. Peroulis, A.K. Bajaj, Dynamics of a nonlinear microresonator based on resonantly interacting flexural-torsional modes, *Nonlinear Dynamics* 54 (1–2) (2008) 31–52.
[27] W.T. Thomson, M.D. Dahleh, *Theory of Vibration with Applications*, Prentice-Hall, Englewood Cliffs, NJ, 1998.
[28] R.G. Jacquot, J.D. Gibson, The effects of discrete masses and elastic supports on continuous beam natural frequencies, *Journal of Sound and Vibration* 23 (2) (1972) 237–244.
[29] R.C. Hibbeler, *Mechanics of Materials*, Pearson Prentice Hall, Upper Saddle River, NJ, 2005.